Towards a Unified Setup to Simulate Mid-Latitude and Tropical Mesoscale Convective Systems at Kilometer-Scales

Andreas Franz Prein[1], Ming Ge[1], Alexandra Nicole Ramos-Valle[2], Dié WANG[3], and Scott Edward Giangrande[3]

[1]National Center for Atmospheric Research (UCAR)
[2]Rutgers University
[3]Brookhaven National Lab

November 21, 2022

Abstract

Mesoscale convective systems (MCSs) are the main source of precipitation in the tropics and parts of the mid-latitudes and are responsible for high-impact weather worldwide. Studies showed that deficiencies in simulating mid-latitude MCSs in state-of-the-art climate models can be alleviated by kilometer-scale models. However, whether these models can also improve tropical MCSs and weather we can find model settings that perform well in both regions is understudied. We take advantage of high-quality MCS observations collected over the Atmospheric Radiation Measurement (ARM) facilities in the U.S. Southern Great Plains (SGP) and the Amazon basin near Manaus (MAO) to evaluate a perturbed physics ensemble of simulated MCSs with 4\,km horizontal grid spacing. A new model evaluation method is developed that enables to distinguish biases stemming from spatiotemporal displacements of MCSs from biases in their reflectivity and cloud shield. Amazon MCSs are similarly well simulated across these evaluation metrics than SGP MCSs despite the challenges anticipated from weaker large-scale forcing in the tropics. Generally, SGP MCSs are more sensitive to the choice of model microphysics, while Amazon cases are more sensitive to the planetary boundary layer (PBL) scheme. Although our tested model physics combinations had strengths and weaknesses, combinations that performed well for SGP simulations result in worse results in the Amazon basin and vice versa. However, we identified model settings that perform well at both locations, which include the Thompson and Morrison microphysics coupled with the Yonsei University (YSU) PBL scheme and the Thompson scheme coupled with the Mellorâ\euro“Yamadaâ\euro“Janjic (MYJ) PBL scheme.

T t t t M t t T M t t t t

rea F. rei[1] i g e[1] le a ra a alle[1] i e a g[2] . i a g ra e[2]

e i

- A
- C US M
- M C

Corresponding author: Andreas F. Prein,

I [illegible] (AR [illegible] & K[illegible] 2008; [illegible] et al., 2017) [illegible] (4 [illegible]) [illegible] MCS [illegible] US D[illegible] E[illegible]s (DOE) [illegible] (ARM) (M[illegible] & [illegible] 2013) [illegible] US [illegible] (SGP [illegible] L[illegible] [illegible] (S[illegible] et al., 2016) [illegible] (MAO) M[illegible] B[illegible] (M[illegible] et al., 2016). MCS [illegible] (2019).

M[illegible] (2019) [illegible] MCS [illegible] SGP [illegible] MAO [illegible] US [illegible] SGP MCS [illegible] MAO MCS (2020). [illegible] SGP MCS [illegible] (e.g., [illegible]), [illegible] MAO MCS [illegible] CRM [illegible] MCS [illegible] MCS [illegible] (2017; F[illegible] et al., 2018; [illegible] et al., 2019; F[illegible] et al., 2017; H[illegible] et al., 2019) [illegible] (BL) [illegible] & A[illegible] 2014) [illegible] M[illegible] US [illegible] MCS [illegible]

[illegible] MCS [illegible] SGP [illegible] MAO [illegible] al. (2019) [illegible] CRM [illegible] MCS [illegible] AR [illegible] MCS [illegible] (R[illegible] & L[illegible] 2008; A. [illegible] et al., 2013). I[illegible] [illegible] MCS [illegible] SGP [illegible] MAO [illegible] BL-[illegible]

2 [illegible]a [illegible]a a [illegible]e

2.1 [illegible]a e [illegible]ele [illegible]i

MCS [illegible] US [illegible] (F[illegible] et al., 1986; H[illegible] Jr, 2018; [illegible] et al., 2019; H[illegible] & A[illegible] 2019b, [illegible] 2019) [illegible] (F[illegible] et al., 2010, F[illegible] et al., 2018; A. F. [illegible] et al., 2020). US MCS [illegible] (L[illegible] et al., 2021). [illegible] MCS [illegible] (2019). [illegible] MCS [illegible] (CAPE) [illegible] (CIN) [illegible] MCS [illegible] (F[illegible] et al., 2021). E[illegible] MCS [illegible] (A. F. [illegible] et al., 2020).

MCS ... 7, 200 MCS ... 2018; ... 2021) ... 50% ... 2021). MCS ... 2021). ... MCS ... (2014–2015), ... 50% ... 2000–2013 ... 2019) ... MCS ... (2019) ... (2020).

... MCS ... US DOE ARM ... 2013) ... (2016) ... 2014/15 ... (2016, 2017); ... (2017)). ... 16 MCS ... 2019). ... 13 ... MCS ... (4 ... 4 ... MCS ... (e.g., ... MCS ...

2.2 ... ber a i al a a e

... (10– ... 3 GHz) ... MCS ... 2014/15 ... (C. ... 2018). ... 2 ... 480 km $\times$ 480 km ... 500 m ... (CAP) ... 500 m ... 20 km ... 2 km ... 4 km ... 6 km ... 2 km CAPs ... 180 km ... 2.4. ... MCS ... 2017) ... US ... 88D ... 2018). ... 0.02° ... 1995 ... 2018 ... MCS ... US ... NEXRAD ... 1–2 ... z ... 2019).

... GOES-13 ... 4 ... 2018). ... 4 ... 1.37 μm ... (Feng ... 2021). ... GOES-13 ... GOES-15 ... June 5, 2013, MCS ... GOES-13. GOES ... 0.04°.

2.3

[illegible] 1. 5- [illegible] B L [illegible] [illegible] (e g, [illegible]) [illegible] (C[illegible], 2013). [illegible] M[illegible], [illegible] M[illegible]N2 [illegible]

2.4 el alua i

[illegible] (e g, [illegible]) [illegible]. [illegible] M C S [illegible] [illegible] fi[illegible] [illegible] M C S [illegible]

In Fig. 2, [illegible] I [illegible] (N), [illegible] $\sim$180 km [illegible] 2 [illegible]. A [illegible] N = 2. 6° ($\sim$290 km) [illegible] ZCAR [illegible] 2 km 4 km [illegible] 6 [illegible] B T [illegible] M C S [illegible]

N[illegible] ([illegible] T) [illegible] T $\pm$ 4 [illegible] M C S [illegible] T [illegible] M C S [illegible] M C S [illegible] 2 ° [illegible] (M = N + 2 ° + 2°; Fig. 2).

F[illegible] (t = 10- [illegible] n, [illegible] B T [illegible] 65 $\times$ 65 [illegible] 165 $\times$ 165 [illegible] i 100 $\times$ 100 [illegible] F[illegible]

[illegible] (CC; [illegible] 2011)) [illegible] B T [illegible] (ACDFD; [illegible] Fig. 2 [illegible]) [illegible] ACDFD, [illegible] B T [illegible]

[illegible] T $\times$ (M $-$ N) $\times$ (M $-$ N) [illegible] ZCC, B TCC, ZACDFD, [illegible] B TACDFD. [illegible] 180, 000 [illegible] M C S [illegible] $\pm$ 4- [illegible] 10- [illegible] (48- [illegible]) [illegible] 100 $\times$ 100 [illegible] (Δ) [illegible] (Δ [illegible]) [illegible] N[illegible] ACDFD [illegible] CC [illegible]

[illegible]. [illegible] F[illegible] [illegible]

[illegible] MCS [illegible] CAPE, CIN, [illegible] ±15 [illegible] CAPE [illegible] CIN [illegible] 3, 000 [illegible] N [illegible] 750 [illegible] CAPE [illegible] CIN [illegible]

3 e ul

3.1 eali e Te

B [illegible] MCS [illegible] (e.g., [illegible] Fig. 2 in [illegible] (2009)) [illegible] (Z). A [illegible]

- [illegible] MCS [illegible] 4 ° (Fig. 3a). [illegible] 350 km (4 ° [illegible] 36.6 ° N [illegible]). A [illegible] CC=1 [illegible] ACDFD=0 dBZ [illegible]
- [illegible] (Fig. 3b) [illegible] 10 dBZ [illegible] (CC=1) [illegible] ACDFD [illegible] 6 dBZ [illegible] 10 dBZ [illegible] dBZ [illegible]
- [illegible] (Fig. 3c) [illegible] 5 ° [illegible] MCS [illegible] 579.2 km (6.6 °) [illegible] CC [illegible] 0.58 [illegible] MCS [illegible] ACDFD [illegible] 6 dBZ [illegible]
- [illegible] (Fig. 3d) [illegible] 7 ° [illegible] 90 °. [illegible] (CC=0.1), [illegible] ACDFD [illegible] Z [illegible]

3.2 alua i i ula e

[illegible] MCS [illegible] MAO [illegible] Fig. 4 [illegible] J [illegible] 6, 2014 [illegible] 9:00 UTC [illegible] MCS [illegible] (Fig. 4a) [illegible] (Fig. 4g). [illegible] (Fig. 4b) [illegible] 4 km [illegible] (Fig. 4h). [illegible] MCS [illegible] 180 km [illegible] Fig. 4a, b)

120 (Fig. 4) n. B (Fig. 4) (Fig. 4) (Fig. 4 ACDFD=7.2K), CC=0.41 (Fig. 4). (Fig. 4) CC 0.54 (Fig. 4) ; (Fig. 4 ACDFD=3.9 B Z.

Fig. 4 ACDFD Z ACDFD B T ZCC, B TCC 10- n N ACDFD B TCC t=0 n E 120 MCS Fig. 4 t=120- n Fig. 4 MCS

3.3 el i e i i i i e

Fig. 5 Nov 17, 2014, MCS MAO B L n Z (Fig. 5). MCS C MXN2 5 B L n MXN2 5 n M n,

Fig. 6 ' n MCS ZCAR 2 . n (. B T (e.g., SPan Jul 18, 2016) Z ACDFD pt MAO SP MCS SP MCS n H SP MCS MCS ( ) ACDFD Z MAO MCS SP (i.e., Z n. SP MCS (, MAO MCS T Z ( ). CC SP 4 kCARs H ACDFD Z (W (Z n n Z n

D[illegible] 2 km, 4 km [illegible] 6 km [illegible] (Fig. 7). L[illegible] MKN2 5 [illegible] B T CCs [illegible] MAO MCSs (Fig. 7b). [illegible] Fig. 5. I[illegible] (Fig. 7c) [illegible] (Fig. 7a).

A[illegible] (D[illegible] 2007; A. F. [illegible], 2011) [illegible] in Fig. 8. C[illegible] (Fig. 8[illegible]). [illegible] B L [illegible] B L [illegible] ~20% [illegible] ACDFD [illegible] B T[illegible] (Fig. 8g), [illegible] ZACDFD [illegible] (Fig. 8f). [illegible] in Fig. 8 [illegible] ACDFD [illegible] (Fig. 8e, f) [illegible] MAO [illegible] (Fig. 8i–l).

[illegible] (Fig. 8m–x). [illegible] MAO [illegible] MCS [illegible] B L [illegible] CC (45%; Fig. 8o) [illegible] ACDFD [illegible] (80%; Fig. 8s). [illegible] ZACDFD [illegible] (60%; Fig. 8r) [illegible] ZCCs [illegible] (60%; Fig. 8n). C[illegible] B T ACDFD [illegible] MAO [illegible]

[illegible] MCSs in [illegible] MAO [illegible] CAPE, CIN, [illegible] (Fig. 9). [illegible] MAO [illegible] MCSs [illegible] CIN [illegible] MKN2 5 B L [illegible] (Fig. 9c). [illegible] MKN2 5 [illegible] B L [illegible] Fig. 5. [illegible] CAPE [illegible] MCSs [illegible] MKN2 5, [illegible] CIN (Fig. 9a). [illegible] CAPE [illegible] CIN [illegible] MCSs (Fig. 9b, d) [illegible] MCSs [illegible] CAPE, [illegible] M[illegible]

[illegible] MKN2 5 [illegible] MAO [illegible] ~3 k[illegible] MCSs [illegible] MCSs [illegible] (Fig. 9e, f), [illegible] C[illegible] MKN2 5 [illegible] B L. [illegible] MCSs (Fig. 9[illegible]).

3.4 [illegible]

I[illegible]

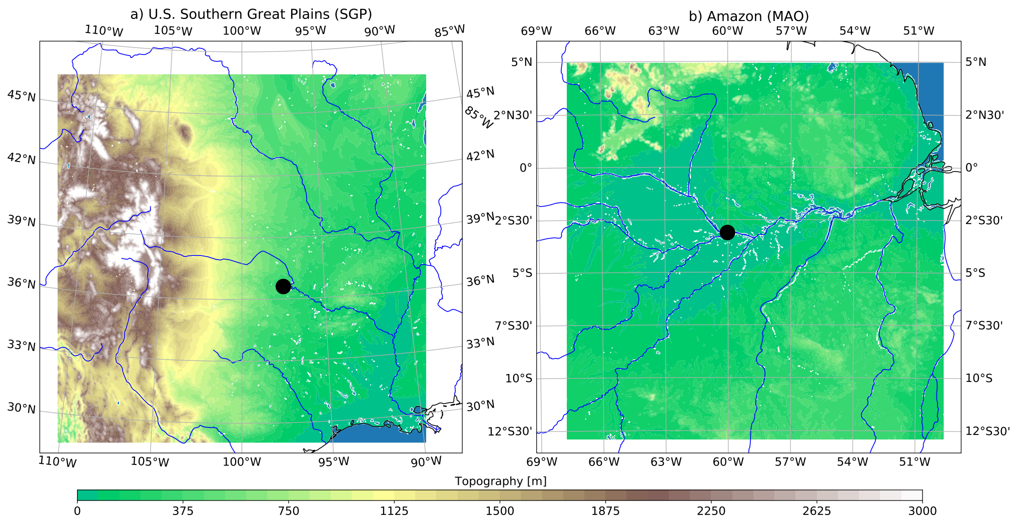

Computational 4 km WRF domains for simulating MCS cases in the U.S. Southern Great Plains (SGP; a) and Amazon basin (MAO; b). The colored contours show the model topography. Each domain consists of 500×500×96 grid cells. The black circle shows the location of the ARM SGP and MAO site.

[illegible]

- [illegible]
- [illegible]

[illegible]

[illegible]

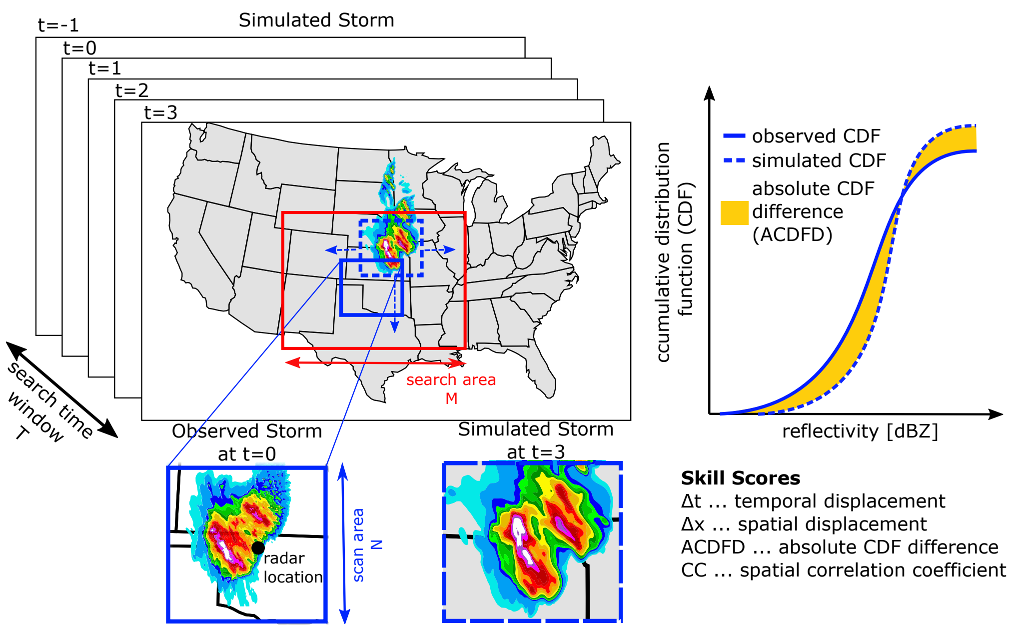

Schematic showing the evaluation framework. An observed storm that passes over a target location (here the SGP ARM site) is defined at time = 0 or $_0$ (lower left corner) within a scan area (; e.g. areal extend of a radar station). A search time window ( ) and search area (; red rectangle in the large map) are defined. Simulated data are derived within the search time window ($_0$ − 2 $_0$ + 2) and within the search area . Two scores are calculated for all possible shifts of the scan area within the search area and every time step ((−) × (−) × combinations for each score). The scores are the spatial correlation coefficient (CC) and the absolute cumulative distribution function difference (ACDFD; orange area in right figure).

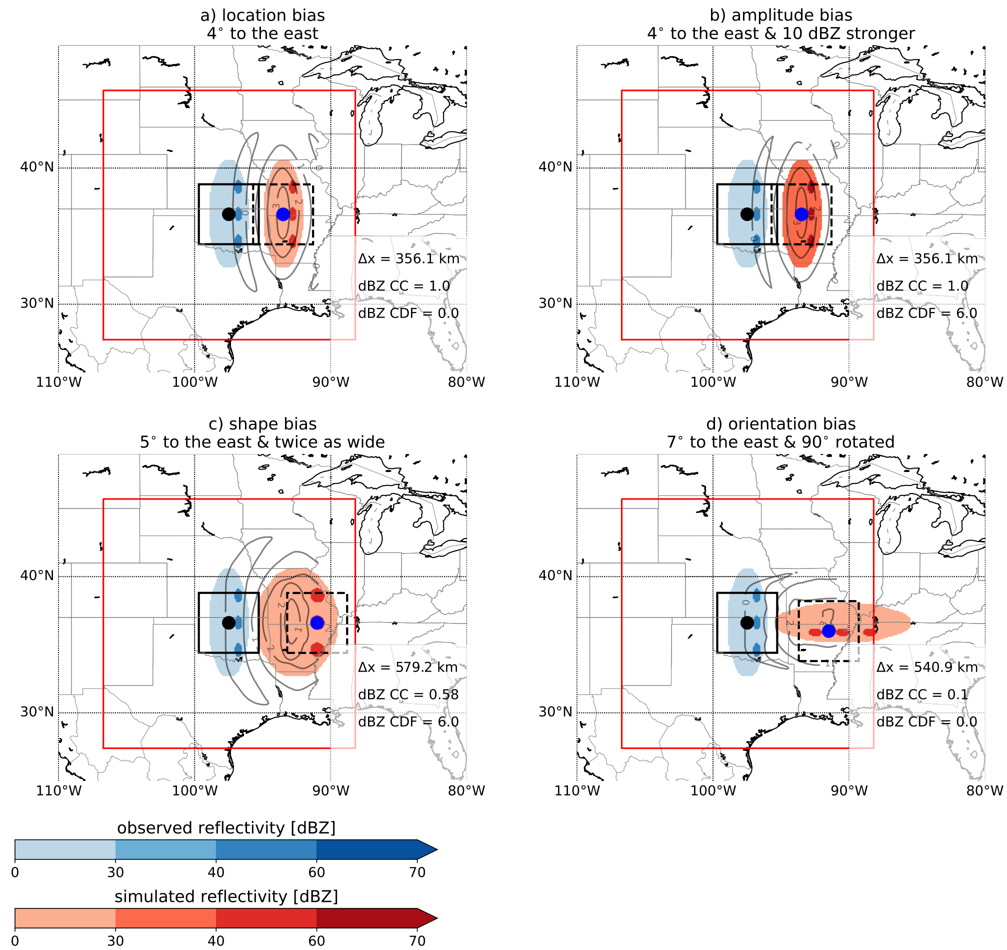

Ideal test case experiment showing the impact of displacements (a), intensity (b), shape (c), and rotational biases (d) on the spatial displacement (Δx), correlation coefficient (CC), and absolute cumulative distribution differences (CDF) skill score between an observed (blue) and simulated (red) storm system. The red rectangle shows the algorithm's search area (=14 degrees), the hypothetical location of a radar site (here the ARM SGP site), the approximate reach of an S-Band radar (black) rectangle (4.4 degrees), displacement matrix (gray contour lines), and the optimal displacement location (blue circle and black dashed rectangle).

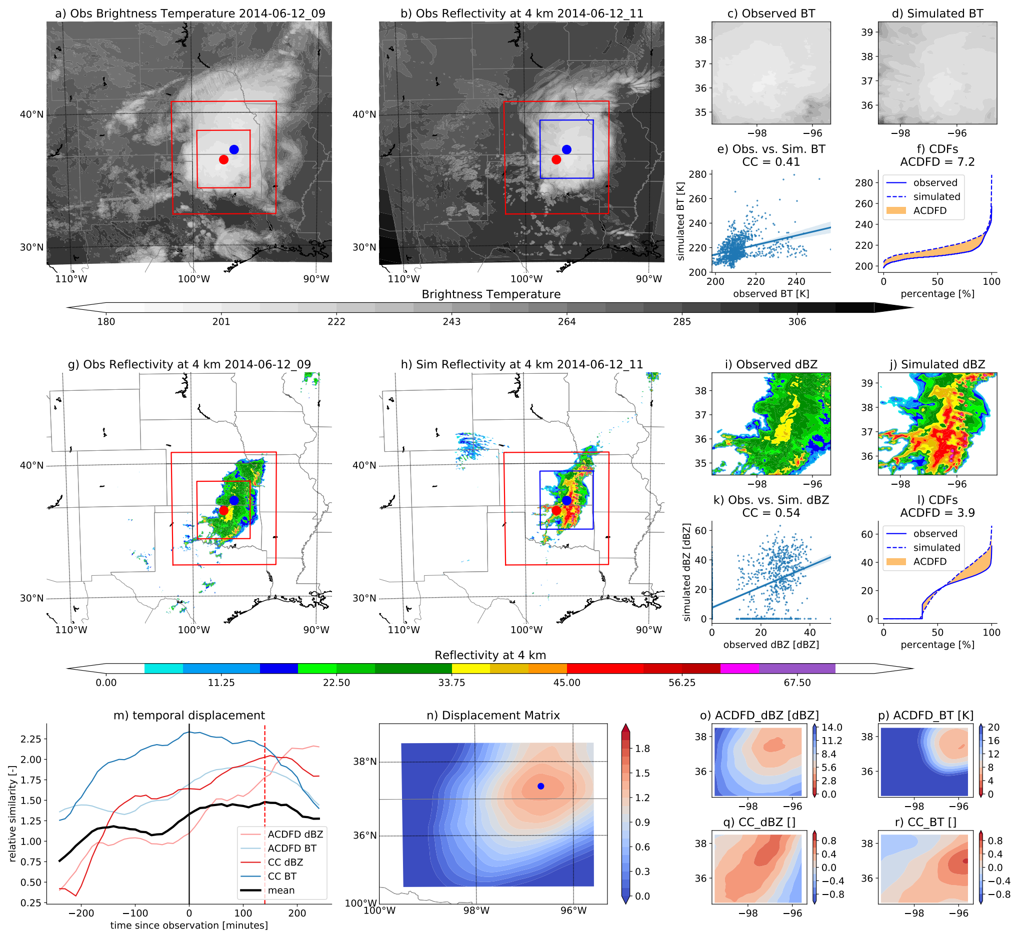

Observed brightness temperature (BT in K; a) and reflectively (Z in dBZ; g) field during an MCS overpass over the ARM SGP site (red dot in a,b,g,h) on June 12, 2014, 9 UTC. Simulated BT (b) and Z (h) field that is most similar to the observed fields using the Thompson microphysics and the YSU PBL scheme. a,b,g,h) The large red rectangle shows the search area and the small red rectangle the scan area. The blue rectangle in b,h shows the most similar simulated area compared to the observed scan area with the blue dot indicating the best estimate for the displacement error. Additionally shown is a zoomed-in version of the observed scan area and the most similar simulated BT (c,d) and Z (i,j). The scatter plot and Spearman correlation coefficient (CC) are shown for BT (c) and Z (k). Only every tenth point is shown in the scatter plot to improve visibility. The absolute commutative distribution differences (ACDFD; orange area) are shown for BT (f) and Z (l). m) Maxima of the normalized spatial fields of Z ACDFD (light red), BT ACDFD (light blue), Z CC (dark red), and BT CC (dark blue). The maxima of the averaged normalized spatial field of these four components is shown as a thick black line and the time displacement (peak value) of the simulated optimal field (120-minutes too late) is indicated with a red dashed line. n) Displacement matrix with the optimal simulated location shown as a blue circle and the four components of the displacement matrix including o) Z ACDFD, p) BT ACDFD, q) Z CC, and r) BT CC during the optimal displacement time.

Figure 5. Example of the observed (a) and simulated (b{j) BT (gray contorts) and radar re ectively (inlet in lower left) at 2 km for the Nov. 17, 2014, MCS case in the Amazon. Results using the Thompson, Morrison, and P3 microphysics scheme are shown top down and YSU, MYJ, and MYNN2.5 planetary boundary layer scheme from left to right.

Acknowledgments

[illegible] DE-[illegible]. S [illegible] LLC, [illegible] DE-[illegible] US DE. [illegible] (ARI) [illegible] a US D[illegible] (DE) [illegible] B[illegible] [illegible] (d 10. 5065/D6[illegible]) [illegible] NCAR s C[illegible] [illegible] No. 1852977. [illegible] L[illegible] DE [illegible] DE-AC02-06CH11357. ERA5 [illegible] ([illegible]). GEOS3 [illegible] GEOS5 [illegible] . GRDAPD [illegible] 4 1.0/ . [illegible] 2014/15 [illegible] ARI s [illegible] . [illegible] WRF . [illegible] A [illegible] U[illegible] _S[illegible] _to _S[illegible] _M[illegible] _T[illegible] _MCSs.

References

A[illegible], S., D[illegible], S., K[illegible], E., B[illegible], O., [illegible] W. S., [illegible], M., ... [illegible] (2018). [illegible] NE[illegible] NOAA s Big Data [illegible], *9* (1), 189-204.

A[illegible], E. M., M[illegible], L. A., [illegible], C., & K[illegible], G. N. (2021). [illegible] L[illegible]

B[illegible], S., K[illegible], E. J., C[illegible], S. C., B[illegible], N., L[illegible], D., [illegible] C., & F[illegible] G. (2020). [illegible], *5* (1), 35-59.

C[illegible], P., [illegible] R. N., L[illegible], H., B[illegible], S. P., & C[illegible] P. C. (2016). [illegible], *3* (2), 165-181.

C[illegible], M. C., C[illegible] Jr, J., M[illegible], P. T., & K[illegible], F. (2013). [illegible], *8* (3), 842-862.

D[illegible], C. A., B[illegible], B. G., B[illegible], R., & H[illegible] G[illegible], J. (2009). [illegible] (MODE) [illegible] 2005 NSL/SPC [illegible], *2* (5), 1252-1267.

D[illegible], M., [illegible], D., [illegible] D., G[illegible], F., C[illegible], J., [illegible], B., ... [illegible] H[illegible], B. (2007). [illegible], *8* (1), 53-70.

D[illegible], L. J., O'B[illegible], T. A., [illegible], D., [illegible], B., & C[illegible], W. F. (2016). [illegible], *6* (20), 12983-12992.

F[illegible], J., H[illegible], B., [illegible], A., M[illegible], H., N[illegible], K., K[illegible], P., ... [illegible] (2017).

[illegible] MC3E [illegible] P I-C[illegible] [illegible], [illegible] (17), 9351–9378.

F[illegible] Z., L[illegible] L. R., H[illegible] S., H[illegible] R. A., B[illegible] C. D., & B[illegible] K. (2016). M[illegible] *[illegible]*, 7(1), 1–18.

F[illegible] Z., L[illegible] L. R., H[illegible] Jr., R. A., H[illegible] S., H[illegible] J., [illegible] Y. Q., . . . F[illegible] J. (2018). [illegible] U S [illegible] *[illegible]*, [illegible] (7), 1470–1494.

F[illegible] Z., L[illegible] L. R., Li[illegible] N., [illegible] W. J., H[illegible] Jr., R. A., Li[illegible] J., . . . G[illegible] J. (2021). A [illegible] U S [illegible] T [illegible] P [illegible] T *[illegible]*, [illegible] (8), 2020JD034202.

F[illegible] Z., [illegible] F., [illegible] K., & L[illegible] L. R. (2021). F[illegible] M[illegible] MAS CA M[illegible] *[illegible]*, [illegible] (7), 2611–2633.

F[illegible] J., K[illegible] R., & C[illegible] C. (1986). [illegible] *[illegible]*, [illegible] (10), 1333–1345.

G[illegible] S. E., F[illegible] Z., J[illegible] M. P., C[illegible] J. M., J[illegible] K. L., [illegible] T. T., . . . [illegible] (2017). C[illegible] M[illegible] G[illegible] O A[illegible] (G[illegible] 2014/5) [illegible] *[illegible]*, [illegible] (23), 14519–14541.

G[illegible] S. E., [illegible] W. D., & M[illegible] D. B. (2020). C[illegible] A[illegible] B [illegible] G[illegible] 2014/5 [illegible] *[illegible]*, [illegible] (12), 7489–7507.

H[illegible] A. M., & A[illegible] W. S. (2019a). C[illegible] *[illegible]*, [illegible] (2), 1144–1153.

H[illegible] A. M., & A[illegible] W. S. (2019b). A[illegible] *[illegible]*, [illegible] (5), 1591–1606.

H[illegible] B., F[illegible] J., [illegible] V. A., M[illegible] H., [illegible] W. C. R., C[illegible] B., . . . [illegible] (2019). C[illegible] MC3E [illegible] P I. [illegible] *[illegible]*, [illegible] (2), 1090–1117.

H[illegible] H., B[illegible] B., B[illegible] P., H[illegible] S., H[illegible] A., [illegible] J., . . . [illegible] (2020). [illegible] *[illegible]*, [illegible] (730), 1999–2049.

H[illegible] C. R., & B[illegible] K. P. (2017). *[illegible]* (H[illegible] R). [illegible] p://[illegible] G[illegible] 3.1-A[illegible]

H[illegible] S.-Y., N[illegible] Y., & D[illegible] J. (2006). A[illegible] *[illegible]*, [illegible] (9), 2318–2341.

H[illegible] S.-Y., & [illegible] H.-L. (1996). N[illegible] *[illegible]*, [illegible] (10), 2322–2339.

H[illegible] Jr., R. A. (2018). 100 [illegible] *[illegible]*, [illegible], 17.1–.

I[illegible] M. J., D[illegible] J. S., M[illegible] E. J., [illegible] M. W., C[illegible] S. A., & C[illegible] W. D. (2008). [illegible]

[illegible], 3 (D13).
J[illegible], Z. I. (1994). [illegible] 2 (5), 927–945.
J[illegible], A. A., H[illegible], J. Y., M[illegible], H., & M[illegible], J. A. (2017). [illegible] 7 (6), 2081–2104.
K[illegible], K. R., & [illegible], S. L. (2018). [illegible] 0 (3), 1417–1425.
Li, J., F[illegible], Z., [illegible], Y., & L[illegible], L. R. (2021). [illegible] 2004–2017. [illegible] 3 (2), 827–856.
Li, G., J[illegible], C. R., L[illegible], L. R., F[illegible], Z., & [illegible], M. (2022). [illegible] 4 (1), 2021MS002660.
Li, C., I[illegible], K., [illegible], R., B[illegible], M., N[illegible], A. J., [illegible], A. F., ... [illegible] (2017). [illegible] 9 (1), 71–95.
M[illegible], S. T., A[illegible], P., M[illegible], L., M[illegible], A. O., [illegible], R. d., [illegible], C., ... [illegible] (2017). [illegible] 14/5) [illegible] 8 (5), 981–997.
M[illegible], S. T., A[illegible], P., M[illegible], L. A. T., M[illegible], A. O., [illegible], R. A. F. d., [illegible], C., ... [illegible] (2016). [illegible] 14/5). [illegible] 6 (8), 4785–4797.
M[illegible], J. H., & [illegible], J. W. (2013). [illegible] 2 (3), 377–392.
M[illegible], G. L., & [illegible], T. (1982). [illegible] 0 (4), 851–875.
M[illegible], F. (1993). [illegible] 5 [illegible].
M[illegible], H., & M[illegible], J. A. (2015). [illegible] 2 (1), 287–311.
M[illegible], H., [illegible], G., & [illegible], V. (2009). [illegible] 7 (3), 991–1007.
N[illegible], M., & N[illegible], H. (2006). [illegible] 3 [illegible] 9 (2), 397–407.
N[illegible], M., & N[illegible], H. (2009). [illegible] 8 (5), 895–912.
NCEP. (2020). [illegible] (NCEP). [illegible] https://dtcenter.org/community-code/unified-post-processor-upp/documentation
N[illegible], S. W., C[illegible], R., & [illegible], S. A. (2006). [illegible] 4 (10), 2702–2721.
N[illegible], G.-Y., [illegible], Z.-L., M[illegible], K. E., C[illegible], F., E[illegible], M. B., B[illegible], M., ... [illegible]

[illegible] (2011). [illegible] ([illegible] MP: 1. M[illegible] [illegible] *[illegible]*, *[illegible]* (D12).

[illegible] B., [illegible] S.-Y. S., Lin, Y.-H., [illegible] L., & [illegible] R. (2018). D[illegible] [illegible] (J[illegible] 2016) [illegible] *[illegible]*, 8.

[illegible] J. G., K[illegible] J. B., [illegible] W. C., D[illegible] C. A., D[illegible] J., G[illegible] D. O., ... [illegible] (2017). [illegible] *[illegible]*, *9* (8), 1717–1737.

[illegible] A., G[illegible] A., [illegible] M., [illegible] H., A[illegible] N., K[illegible] K., & G[illegible] G. (2013). A[illegible] *[illegible]*, *4* (9-10), 2653–2677.

[illegible] A. F., G[illegible] A., & [illegible] H. (2011). A[illegible] [illegible] E[illegible] *[illegible]*, *[illegible]* (4), 383.

[illegible] A. F., L[illegible] W., F[illegible] G., F[illegible] A., B[illegible] N., G[illegible] K., ... [illegible] (2015). A[illegible] D[illegible] *[illegible]*, *3* (2), 323–361.

[illegible] A. F., Liu, C., I[illegible] K., B[illegible] R., [illegible] R. M., H[illegible] G. J., & C[illegible] M. (2020). [illegible] *[illegible]*, *5* (1), 95–110.

[illegible] A. F., Liu, C., I[illegible] K., [illegible] S. B., [illegible] R. M., H[illegible] G. J., & C[illegible] M. P. (2017). I[illegible] [illegible] *[illegible]*, *7* (12), 880–884.

[illegible] K. L., [illegible] M. D., & H[illegible] Jr, R. A. (2014). [illegible] *[illegible]*, *4* (20), 7359–7366.

[illegible] A., A[illegible] T., & M[illegible] C. R. (2018). M[illegible] [illegible] A[illegible] [illegible]: [illegible] *[illegible]*, *8* (1), 215–229.

[illegible] A., A[illegible] T., M[illegible] C. R., E[illegible] S. A., & M[illegible] T. A. (2019). M[illegible] A[illegible] [illegible] 2014/5 [illegible] *[illegible]*, *9* (15), 5599–5618.

[illegible] N. M., & L[illegible] H. W. (2008). [illegible] *[illegible]*, *[illegible]* (1), 78–97.

[illegible] M., [illegible] B., J[illegible] F., K[illegible] M., Lin, S.-J., [illegible] W. M., & [illegible] P. (2019). G[illegible] *[illegible]*, *5* (3), 172–184.

[illegible] C., & F[illegible] A. (2018, 4). *[illegible]* *[illegible]* ([illegible]). [illegible] N[illegible] L[illegible] ([illegible]L).

[illegible] R. S., & J[illegible] R. H. (2005). [illegible] *[illegible]*, *3* (4), 961–976.

[illegible] J., K[illegible] A., L[illegible] B., F[illegible] J., H[illegible] B., [illegible] A., ... G[illegible] D. (2019). [illegible] [illegible] 1: H[illegible] *[illegible]*, *[illegible]* (24), 14072–14101.

[illegible] D., [illegible] R., C[illegible] T., L[illegible] P., & [illegible] D. (2016). [illegible] ([illegible]) *[illegible]*, *7*, 64.

Skamarock, W. C., & Klemp, J. B. (2008). A time-split nonhydrostatic atmospheric model for weather research and forecasting applications. Journal of computational physics, 227(7), 3465–3485.
Song, F., Feng, Z., Leung, L. R., Houze Jr, R. A., Wang, J., Hardin, J., & Homeyer, C. R. (2019). Contrasting spring and summer large-scale environments associated with mesoscale convective systems over the US Great Plains. Journal of Climate, 32(20), 6749–6767.
Stephan, C., & Alexander, M. J. (2014). Summer season squall-line simulations: Sensitivity of gravity waves to physics parameterization and implications for their parameterization in global climate models. Journal of the Atmospheric Sciences, 71(9), 3376–3391.
Stevens, B., Satoh, M., Auger, L., Biercamp, J., Bretherton, C. S., Chen, X., . . . others (2019). DYAMOND: the DYnamics of the Atmospheric general circulation Modeled On Non-hydrostatic Domains. Progress in Earth and Planetary Science, 6(1), 1–17.
Thompson, G., Rasmussen, R. M., & Manning, K. (2004). Explicit forecasts of winter precipitation using an improved bulk microphysics scheme. Part I: Description and sensitivity analysis. Monthly Weather Review, 132(2), 519–542.
Trier, S., Davis, C., & Ahijevych, D. (2010). Environmental controls on the simulated diurnal cycle of warm-season precipitation in the continental United States. Journal of the atmospheric sciences, 67(4), 1066–1090.
Wang, D., Giangrande, S. E., Feng, Z., Hardin, J. C., & Prein, A. F. (2020). Updraft and downdraft core size and intensity as revealed by radar wind profilers: MCS observations and idealized model comparisons. Journal of Geophysical Research: Atmospheres, 125(11), e2019JD031774.
Wang, D., Giangrande, S. E., Schiro, K. A., Jensen, M. P., & Houze Jr, R. A. (2019). The characteristics of tropical and midlatitude mesoscale convective systems as revealed by radar wind profilers. Journal of Geophysical Research: Atmospheres, 124(8), 4601–4619.
Wilks, D. S. (2011). Statistical methods in the atmospheric sciences (Vol. 100). Academic press.
Wu, X., & Yan, J. (2011). Estimating the outgoing longwave radiation from the FY-3B satellite visible infrared radiometer Channel 5 radiance observations. Chinese Science Bulletin, 56(32), 3480–3485.
Xue, L., Fan, J., Lebo, Z. J., Wu, W., Morrison, H., Grabowski, W. W., . . . others (2017). Idealized simulations of a squall line from the MC3E field campaign applying three bin microphysics schemes: Dynamic and thermodynamic structure. Monthly Weather Review, 145(12), 4789–4812.
Yang, G.-Y., & Slingo, J. (2001). The diurnal cycle in the tropics. Monthly Weather Review, 129(4), 784–801.